

See discussions, stats, and author profiles for this publication at: <https://www.researchgate.net/publication/221797359>

# Uranyl Peroxide Oxalate Cage and Core-Shell Clusters Containing 50 and 120 Uranyl Ions

ARTICLE in INORGANIC CHEMISTRY · FEBRUARY 2012

Impact Factor: 4.76 · DOI: 10.1021/ic202380g · Source: PubMed

CITATIONS

28

READS

18

## 3 AUTHORS:



Jie Ling

University of Notre Dame

53 PUBLICATIONS 805 CITATIONS

SEE PROFILE



Jie Qiu

University of Notre Dame

23 PUBLICATIONS 372 CITATIONS

SEE PROFILE



Peter C Burns

University of Notre Dame

490 PUBLICATIONS 8,273 CITATIONS

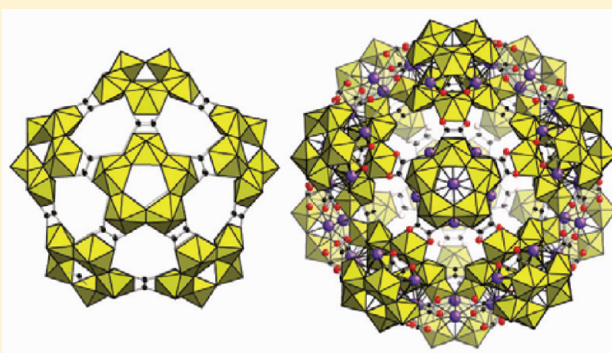
SEE PROFILE

## Uranyl Peroxide Oxalate Cage and Core–Shell Clusters Containing 50 and 120 Uranyl Ions

Jie Ling,<sup>†</sup> Jie Qiu,<sup>†</sup> and Peter C. Burns<sup>\*,†,‡</sup><sup>†</sup>Department of Civil Engineering and Geological Sciences, University of Notre Dame, Notre Dame, Indiana 46556, United States<sup>‡</sup>Department of Chemistry and Biochemistry, University of Notre Dame, Notre Dame, Indiana 46556, United States

## S Supporting Information

**ABSTRACT:** Cage clusters built from uranyl hexagonal bipyramids and oxalate ligands crystallize from slightly acidic aqueous solution under ambient conditions, facilitating structure analysis. Each cluster contains uranyl ions coordinated by peroxo ligands in a bidentate configuration. Uranyl ions are bridged by shared peroxo ligands, oxalate ligands, or through hydroxyl groups.  $\text{U}_{50}\text{Ox}_{20}$  contains 50 uranyl ions and 20 oxalate groups and is a topological derivative of the  $\text{U}_{50}$  cage cluster that has a fullerene topology.  $\text{U}_{120}\text{Ox}_{90}$  contains 120 uranyl ions and 90 oxalate groups and is the largest and highest mass cluster containing uranyl ions that has been reported. It has a core–shell structure, in which the inner shell (core) consists of a cluster of 60 uranyl ions and 30 oxalate groups, identical to  $\text{U}_{60}\text{Ox}_{30}$ , with a fullerene topology. The outer shell contains 12 identical units that each consist of five uranyl hexagonal bipyramids that are linked to form a ring (topological pentagon), with each uranyl ion also coordinated by a side-on nonbridging oxalate group. The five-membered rings of the inner and outer shells (the topological pentagons) are in correspondence and are linked through K cations. The inner shell topology has therefore templated the location of the outer shell rings, and the K counterions assume a structure-directing role. Small-angle X-ray scattering data demonstrated  $\text{U}_{50}\text{Ox}_{20}$  remains intact in aqueous solution upon dissolution. In the case of clusters of  $\text{U}_{120}\text{Ox}_{90}$ , the scattering data for dissolved crystals indicates the  $\text{U}_{60}\text{Ox}_{30}$  core persists in solution, although the outer rings of uranyl bipyramids contained in the  $\text{U}_{120}\text{Ox}_{90}$  core–shell cluster appear to detach from the cluster when crystals are dissolved in water.



## ■ INTRODUCTION

Polyoxometalates have been intensely studied because of their remarkable compositional and structural diversity and potential application in catalysis, nanotechnology, biomedicine, and materials science.<sup>1–11</sup> Polyoxometalates are mainly based on group V and VI transition metals and have only relatively recently been extended into the actinide elements. Duval reported uranium-based clusters with a polyoxometalate core containing six U(V) cations.<sup>12</sup> Soderholm reported the synthesis and structure of a Pu(IV) oxide cluster containing 38 Pu cations.<sup>13</sup> We earlier reported clusters that are built from U(VI) uranyl polyhedra that contain from 16 to 60 uranyl ions.<sup>14–23</sup> Within these clusters, uranyl cations are connected by sharing peroxide or hydroxyl groups within the equatorial plane of their corresponding hexagonal bipyramids. The result is a series of open and cage clusters that are 1.5–3 nm in diameter. The topologies of the cage clusters are highly varied and are based on combinations of topological squares, pentagons, and hexagons. Several adopt fullerene topologies, including  $\text{U}_{60}$  that is topologically identical to  $\text{C}_{60}$ .<sup>20</sup>

Quantum mechanical simulations indicate that a bent  $\text{U}-(\text{O}_2)-\text{U}$  interaction is energetically favored over a  $180^\circ$  dihedral angle, owing to a partially covalent interaction between

the  $\text{U}^{6+}$  cation and the peroxo ligand.<sup>24,25</sup> The bent configuration encourages self-assembly of uranyl ions into cage clusters, rather than extended structural units such as sheets that dominate the solid state chemistry of uranyl compounds. We recently expanded the family of uranyl peroxide cage clusters by incorporating pyrophosphate and oxalate ligands.<sup>16,17</sup> The size, topologies, cavities, and pore spaces of clusters built from uranyl polyhedra differ significantly and to some extent can be selected by controlling solution pH, reaction stoichiometry, and the counterions available.

Expanding upon our earlier work, we continue to study the reaction of uranyl nitrate with peroxide and oxalate under ambient conditions in water. We have crystallized two new cluster types in good yield. These clusters are designated  $\text{U}_{50}\text{Ox}_{20}$  and  $\text{U}_{120}\text{Ox}_{90}$ , where U and Ox represent uranyl and oxalate, respectively, and the subscripts give the quantities of each in the cluster. Note that the latter cluster contains 120 uranyl ions, twice as many as the largest previously reported cluster.

Received: November 2, 2011

Published: February 1, 2012

## EXPERIMENTAL SECTION

**Synthesis. Caution:** Although isotopically depleted uranium was used for all experiments described here, appropriate precautions are essential for handling all radioactive materials.

Following our initial report of the self-assembly of uranyl peroxo polyhedra into cage clusters in 2005,<sup>14</sup> we have conducted an extensive combinatorial synthesis program aimed at expanding this family of nanoscale materials. This approach provided a family of more than 30 reported clusters with varied topologies and sizes. In general, our approach has focused on varying solution pH and counterions in solution. Whereas cage clusters built from uranyl peroxo polyhedra alone have only been synthesized under alkaline conditions, providing units such as oxalate or pyrophosphate that can bridge between uranyl ions has extended the pH range of cluster assembly, as well as the topological and compositional complexity of the resulting clusters. The syntheses methods provided here reproducibly provide crystals containing one of two uranyl peroxo oxalate cage clusters.

**U<sub>50</sub>Ox<sub>20</sub>.** Crystals containing U<sub>50</sub>Ox<sub>20</sub> were synthesized by loading UO<sub>2</sub>(NO<sub>3</sub>)<sub>2</sub>·6H<sub>2</sub>O (0.5 M, 0.1 mL), H<sub>2</sub>O<sub>2</sub> (30%, 0.1 mL), LiOH (2.38 M, 0.1 mL), KCl (0.5 M, 0.05 mL), and H<sub>2</sub>C<sub>2</sub>O<sub>4</sub> (0.5 M, 0.14 mL) in a 2 mL scintillation vial. The initial pH of the resulting solution was 5.2. Yellow needle-like crystals of U<sub>50</sub>Ox<sub>20</sub> formed after two months as the solution was evaporated under ambient conditions. The yield of crystals was ~22% on the basis of uranium. The pH of the solution at the time of crystal harvest was 5.6.

**U<sub>120</sub>Ox<sub>90</sub>.** Crystals containing U<sub>120</sub>Ox<sub>90</sub> were synthesized by loading UO<sub>2</sub>(NO<sub>3</sub>)<sub>2</sub>·6H<sub>2</sub>O (0.5 M, 0.1 mL), H<sub>2</sub>O<sub>2</sub> (30%, 0.1 mL), LiOH (2.38 M, 0.1 mL), KCl (0.5 M, 0.125 mL), and H<sub>2</sub>C<sub>2</sub>O<sub>4</sub> (0.5 M, 0.125 mL) in a 2 mL scintillation vial. The initial pH of the solution was 6.7. Yellow blocky crystals containing U<sub>120</sub>Ox<sub>90</sub> crystallized within a month from the solution that was left standing under ambient conditions. The crystal yield was ~38% on the basis of uranium. The pH of the mother solution when the crystals were harvested was 6.5.

**X-ray Diffraction.** X-ray diffraction was collected for each compound at 110 K using a Bruker goniometer, an APEX II CCD detector, and graphite-monochromated Mo K $\alpha$  radiation from a conventional tube. Semiempirical corrections for absorption were applied to the full sphere of data collected in each case using the program SADABS. Data were integrated using the Bruker APEX II software and the SHELXTL<sup>26</sup> system of programs was used for the solution and refinement of each structure. Selected crystallographic data are presented in Table 1. Details of each structure are in the Supporting Information.

**Table 1. Crystallographic Data for U<sub>50</sub>Ox<sub>20</sub> and U<sub>120</sub>Ox<sub>90</sub>**

formula	U <sub>50</sub> Ox <sub>20</sub>	U <sub>120</sub> Ox <sub>90</sub>
formula mass	18778.20	51698.20
crystal system	orthorhombic	cubic
space group	<i>Cmcm</i>	<i>Im</i> $\bar{3}$
<i>a</i> (Å)	28.152(3)	40.554(4)
<i>b</i> (Å)	42.662(5)	40.554(4)
<i>c</i> (Å)	40.296(4)	40.554(4)
<i>V</i> (Å <sup>3</sup> )	48397(9)	66695(13)
<i>Z</i>	4	2
$\lambda$ (Å)	0.71073	0.71073
$\mu$ (mm <sup>-1</sup> )	16.9	15.0
$\theta$ (deg) range	1.3–22.6	1.2–20.7
$\rho_{\text{calcd}}$ (g cm <sup>-3</sup> )	2.577	2.574
<i>S</i>	1.05	1.13
$R(F)$ for $F_o^2 > 2\sigma(F_o^2)^a$	0.054	0.065
$R_w(F_o^2)^b$	0.1698	0.1982
$^a R(F) = \sum   F_o  -  F_c   / \sum  F_o $ . $^b R_w(F_o^2) = [\sum [w(F_o^2 - F_c^2)^2] / \sum wF_o^4]^{1/2}$ .		

**Chemical Analysis.** Crystals of U<sub>50</sub>Ox<sub>20</sub> and U<sub>120</sub>Ox<sub>90</sub> were harvested and washed lightly using deionized water in a vacuum filter. Crystals were dissolved in nitric acid and the resulting solutions were

analyzed using a Perkin–Elmer ICP-OES. Analysis for three separately washed samples gave consistent U/K/Li ratios of 50:16:8 and 120:134:46 for crystals of U<sub>50</sub>Ox<sub>20</sub> and U<sub>120</sub>Ox<sub>90</sub>, respectively.

Energy dispersive spectra were collected for single crystals containing each cluster using a LEO EVO-50XVP variable-pressure/high-humidity scanning electron microscope. Spectra collected for each compound confirmed the presence of K and U with U/K ratios of 50:17 and 120:130 for U<sub>50</sub>Ox<sub>20</sub> and U<sub>120</sub>Ox<sub>90</sub>, respectively, consistent with the results from ICP-OES. Li cannot be detected using this method.

**Spectroscopy.** Infrared spectra were collected from single crystals of U<sub>50</sub>Ox<sub>20</sub> and U<sub>120</sub>Ox<sub>90</sub> using a SensIR technology IlluminatIR FT-IR microspectrometer. A single crystal of each compound was placed on a glass slide, and the spectrum was collected using a diamond ATR objective. Each spectrum was taken from 650 to 4000 cm<sup>-1</sup> with a beam aperture of 100  $\mu$ m. The spectra for these two compounds, which are shown in the Supporting Information, are virtually identical. In both cases an intense band at ~890 cm<sup>-1</sup> is assigned to the asymmetric stretch of the uranyl units.<sup>27</sup> Asymmetric stretches of oxalate ligands are at ~1344 cm<sup>-1</sup> and ~1615 cm<sup>-1</sup>,<sup>28</sup> with the latter overlapping with a mode due to water bending. H bonding in the compounds is confirmed by a broad band from about 3000 to 3500 cm<sup>-1</sup>.

**Small-Angle X-ray Scattering.** Small-angle X-ray scattering (SAXS) data were collected using a Bruker Nanostar equipped with a Cu microfocus source, Montel multilayer optics, and a HiSTAR multiwire detector. Data were collected with the sample chamber under vacuum and a sample-to-detector distance of 26.3 cm.

SAXS data were collected for clusters introduced into solution by dissolving single crystals of either U<sub>50</sub>Ox<sub>20</sub> and U<sub>120</sub>Ox<sub>90</sub> in ultrapure water. Crystals were isolated from their mother solution by vacuum filtration. They were rinsed gently using water and were harvested from the filter membrane prior to dissolution in ultrapure water. The solutions were drawn into 0.5 mm diameter glass capillaries, and the ends of each capillary were sealed using wax. Water in an identical capillary was used for background measurement.

## RESULTS

The clusters U<sub>50</sub>Ox<sub>20</sub> and U<sub>120</sub>Ox<sub>90</sub> crystallize upon partial evaporation of the corresponding solutions. Structure analyses show that all U atoms in U<sub>50</sub>Ox<sub>20</sub> and U<sub>120</sub>Ox<sub>90</sub> are present as typical (UO<sub>2</sub>)<sup>2+</sup> uranyl U(VI) cations, with U–O bond lengths of ~1.8 Å and U–O–U angles of ~180°.<sup>29</sup>

The structure analysis of U<sub>50</sub>Ox<sub>20</sub> provided the locations of all U atoms, the O atoms that coordinate the U atoms, and the C and O atoms of the oxalate groups. Six K sites corresponding to 12 K cations per U<sub>50</sub>Ox<sub>20</sub> cluster were also located. Li and H atoms were not located in the difference-Fourier maps, owing to their low X-ray scattering efficiencies. The structure contains large areas with significant electron density that we attribute to disordered K, Li and H<sub>2</sub>O or H<sub>3</sub>O. The chemical analysis indicate there are 16 K and eight Li cations per cluster, leading us to assume that there are six H<sub>3</sub>O<sup>+</sup> cations per cluster. Hydroxyl anions and peroxo groups bound to U<sup>6+</sup> cations were identified on the basis of a bond-valence analysis<sup>29</sup> and O–O bond lengths in the case of the peroxo ligands. Crystals containing U<sub>50</sub>Ox<sub>20</sub> have the composition K<sub>16</sub>Li<sub>8</sub>(H<sub>3</sub>O)<sub>6</sub>·[(UO<sub>2</sub>)<sub>50</sub>(O<sub>2</sub>)<sub>43</sub>(OH)<sub>4</sub>(C<sub>2</sub>O<sub>4</sub>)<sub>20</sub>](H<sub>2</sub>O)<sub>*n*</sub>.

U<sub>50</sub>Ox<sub>20</sub> is illustrated in Figure 1, with K cations omitted for clarity. All uranyl ions are present as part of hexagonal bipyramids. Considering for the moment only the uranyl hexagonal bipyramids, there are three types of units in the clusters (Figure 1e, f, g). The simplest of these is a ring consisting of five bipyramids that share peroxo ligands that are bidentate to the uranyl ions (Figure 1e, i). The coordination polyhedron of each uranyl ion is completed by a side-on oxalate



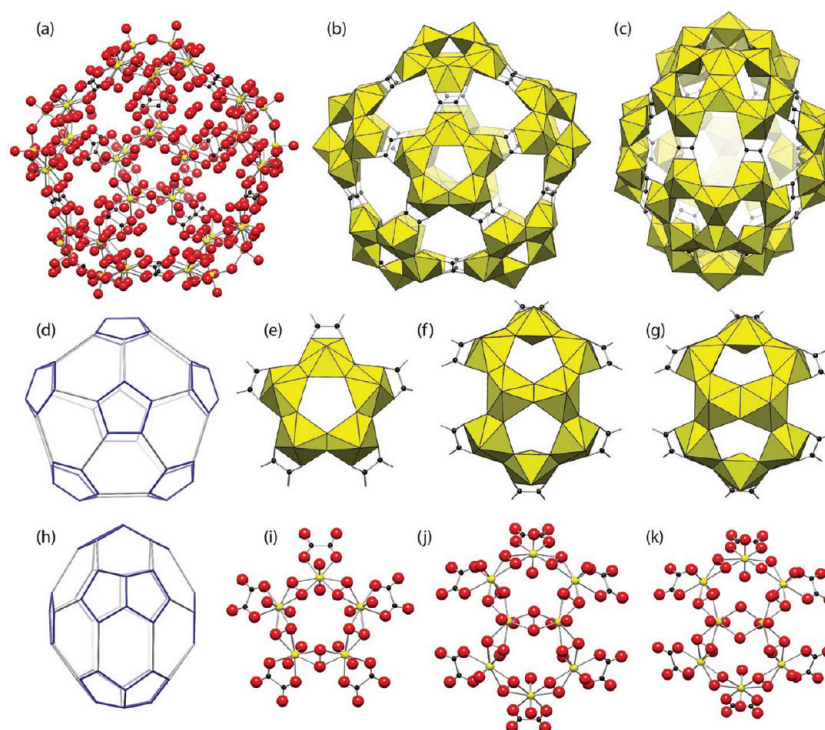


**Figure 1.** Representations of the structure of cluster  $U_{50}Ox_{20}$ . (a–c) Ball-and-stick and polyhedral representations of the cluster, with counterions omitted. (d, h) Graphical representations in which each vertex corresponds to a U cation. Blue lines denote the sharing of polyhedral edges between the corresponding uranyl ions. Gray lines represent linkage of the corresponding uranyl ions through oxalate. (e–g, i–k) Representations of the uranyl polyhedral building units found in  $U_{50}Ox_{20}$ . In all cases uranyl polyhedra are shown in yellow. O, C, and U atoms are shown as red, black, and yellow balls, respectively.

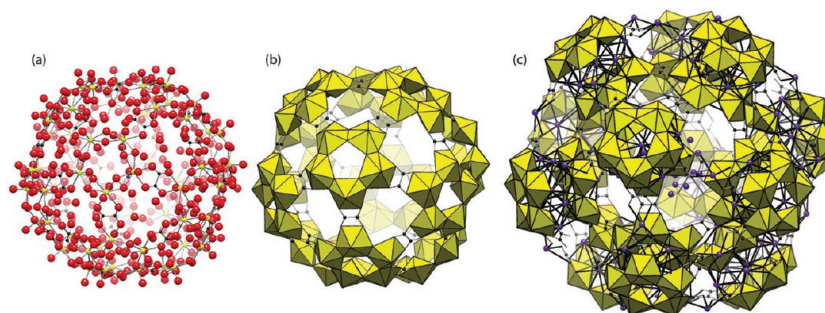


**Figure 2.** Ball-and-stick and polyhedral representations of cluster  $U_{120}Ox_{90}$ . Panels a and b show only the inner shell, which consists of a  $U_{60}Ox_{30}$  cage cluster with a corresponding fullerene topology. Counterions have been excluded. Panel c illustrates the entire cluster, including both shells of uranyl polyhedra, as well as K cation locations (blue balls). Legend as in Figure 1.

group that shares two O atoms with the uranyl polyhedron. The other two units built from uranyl polyhedra each contain eight bipyramids arranged to form two five-membered rings that have two bipyramids in common (Figure 1f, g, j, k). In the unit shown in Figure 1f, all of the edges that are shared between bipyramids correspond to peroxo ligands, and the two central bipyramids share three peroxo ligands with other bipyramids. The coordination polyhedra about the remaining uranyl ions are completed by side-on oxalate groups. The unit shown in Figure 1g differs from that of Figure 1f because the edge shared between the two central bipyramids corresponds to two hydroxyl groups, rather than a peroxo group. The three distinct units consisting of uranyl bipyramids are assembled into a cage cluster by linkages through oxalate groups, such that each oxalate group coordinates two different uranyl ions in side-on

configurations, and each oxalate is shared by two adjacent polyhedra.

Each  $U_{50}Ox_{20}$  cluster contains two simple five-membered rings, shown in Figure 1e, three of the units shown in Figure 1f, and two of those shown in Figure 1g. The cluster has approximate 5-fold rotational symmetry, although the presence of four hydroxyl groups reduces the symmetry to  $2mm$ .

K cations are located within the  $U_{50}Ox_{20}$  cage cluster, inside each five-membered ring of uranyl bipyramids. However, the K sites located below the units shown in Figure 1f, g are separated by only  $\sim 2.5$  Å, indicating that locally one is occupied by K and the other is either vacant or occupied by  $H_2O$ . Refinement of the occupancies of these sites gave 60% against the scattering factor of K, consistent with the presence of  $H_2O$  at these sites where K is absent.

The shape of  $\text{U}_{50}\text{Ox}_{20}$  is a flattened spheroid, with maximum outer diameters of 23.9 and 29.4 Å, as measured from the outer edges of bounding O atoms of uranyl ions. The  $\text{U}-(\text{O}_2)-\text{U}$  dihedral angles range from 137.6 to 144.6°, consistent with previously reported clusters and quantum mechanical simulations.<sup>24,25</sup>

Graphical representations of  $\text{U}_{50}\text{Ox}_{20}$  are provided in Figure 1d, h, where each vertex corresponds to a  $\text{U}^{6+}$  cation. Shared edges between uranyl bipyramids are illustrated by blue lines that connect the corresponding vertices. Where uranyl ions are bridged through oxalate ligands, their corresponding vertices are connected through gray lines.  $\text{U}_{50}\text{Ox}_{20}$  adopts a fullerene topology with 12 pentagons and 15 hexagons and is a derivative of the  $\text{U}_{50}$  cluster topology we reported earlier that contained no oxalate.<sup>15</sup>

The structure analysis of crystals of  $\text{U}_{120}\text{Ox}_{90}$  provided the locations of all U atoms, the O atoms that coordinate the U atoms, and the C and O atoms of the oxalate groups. Eight K sites corresponding to 128 K cations per  $\text{U}_{120}\text{Ox}_{90}$  cluster were located. Li and H atoms were not located. The structure has largely void areas that contain electron density that we attribute to disordered  $\text{H}_2\text{O}$ , K, and Li. Peroxo O atoms were readily identified by their O–O bond lengths. Chemical analysis indicated that for each  $\text{U}_{120}\text{Ox}_{90}$  cluster, there are 134 K cations and 46 Li cations, which balance the charge of the uranyl and oxalate portions of the cluster. The formula of  $\text{U}_{120}\text{Ox}_{90}$ -bearing crystals is  $\text{K}_{134}\text{Li}_{46}[(\text{UO}_2)_{120}(\text{O}_2)_{120}(\text{C}_2\text{O}_4)_{90}](\text{H}_2\text{O})_n$ .

$\text{U}_{120}\text{Ox}_{90}$  is illustrated in Figure 2. The local coordination environments about all the uranyl ions in  $\text{U}_{120}\text{Ox}_{90}$  are identical and consist of two peroxo ligands bidentate to the uranyl ion, with the hexagonal bipyramids completed by a side-on oxalate group. Uranyl bipyramids share peroxo ligands, forming five membered rings of polyhedra analogous to those shown in Figure 1e. There are 24 such five-membered rings in  $\text{U}_{120}\text{Ox}_{90}$ . These are arranged such that the  $\text{U}^{6+}$  cations form a core–shell structure, each with 60 cations. Those in the core are located between 12.30 and 12.32 Å from the center of the cluster, and those of the shell are from 17.94 to 17.99 Å from the center of the cluster. Consider first  $\text{U}^{6+}$  cations in the core. Each uranyl bipyramid belongs to one of 12 five-membered rings of bipyramids. Oxalate ligands bridge directly between uranyl ions belonging to adjacent rings of polyhedra, resulting in a cage that consists of 60 uranyl bipyramids and 30 oxalate groups that is topologically and chemically identical to the  $\text{U}_{60}\text{Ox}_{30}$  cluster we reported earlier. This cage cluster is also topologically identical to  $\text{U}_{60}$  and  $\text{C}_{60}$ .

Continuing to consider only the core of uranyl bipyramids and oxalate ligands, 12 K cations are located inside the cage, one in each of the 12 five-membered rings of uranyl bipyramids (the topological pentagons). The K cations are bonded to each of the five O atoms of uranyl ions emanating from the rings of bipyramids, with bond lengths in the range of ~2.85 Å. There are an additional 20 K cation sites closer to the center of the cage cluster.

The shell in cluster  $\text{U}_{120}\text{Ox}_{90}$  consists of 12 five-membered rings of uranyl hexagonal bipyramids. Unlike the inner core, oxalate ligands do not bridge between uranyl ions. However, the five-membered rings of bipyramids in the shell are linked to adjacent rings through bonds to K cations. The five-membered rings of bipyramids in the shell are each aligned with those of the core, and the pairs of inner and outer rings of bipyramids are linked through six K cations. One of these is located inside

the five-membered ring of bipyramids, whereas the other five are located slightly outside the ring (Figure 3).

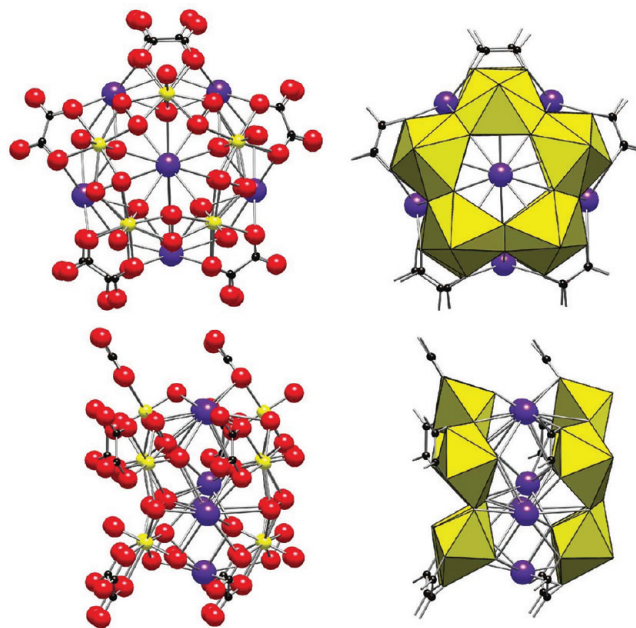


**Figure 3.** Ball-and-stick and polyhedral representations of the K cation locations between five-membered rings of uranyl polyhedra (topological pentagons) of the inner and outer shells of uranyl polyhedra in  $\text{U}_{120}\text{Ox}_{90}$ . Legend as in Figures 1 and 2.

All polyhedral edges that are shared between uranyl ions correspond to peroxo ligands in  $\text{U}_{120}\text{Ox}_{90}$ , and  $\text{U}-(\text{O}_2)-\text{U}$  dihedral angles range from 140.7 to 142.7°. The five-membered rings of bipyramids are oriented similarly in the core and shell; specifically, the rings are concave toward the center of the cluster. The overall cluster has a diameter of 4 nm, as measured from the edges of bounding O atoms.

The SAXS data for solutions created by dissolving crystals of  $\text{U}_{50}\text{Ox}_{20}$  and  $\text{U}_{120}\text{Ox}_{90}$  exhibit scattering in low  $q$  regions (Figure 4). The data for the solution into which  $\text{U}_{50}\text{Ox}_{20}$  crystals were dissolved are readily fit by a core–shell model having inner and outer radii of 5.8 and 14.6 Å (Figure 4a). The outer radius of the flattened  $\text{U}_{50}\text{Ox}_{20}$  cluster derived from the crystallographic study ranges from 12.0 to 14.7 Å, and the SAXS data is consistent with the  $\text{U}_{50}\text{Ox}_{20}$  cluster remaining intact upon dissolution in water. The SAXS data for  $\text{U}_{120}\text{Ox}_{90}$  were fit with a core–shell model with inner and outer radii of 4.7 and 15.7 Å, respectively. The crystallographic radius for the entire cluster is 20.5 Å, whereas that for the inner cluster containing 60 uranyl polyhedra is 15.0 Å. The SAXS data therefore indicate that dissolution of crystals of  $\text{U}_{120}\text{Ox}_{90}$  in small quantities in water causes detachment of the outer five-membered rings of uranyl polyhedra, although the core of the  $\text{U}_{120}\text{Ox}_{90}$  cluster remains intact.

## DISCUSSION

We previously described the synthesis of a family of cage clusters, with fullerene topologies, that are built solely from uranyl polyhedra.<sup>30</sup> In these, uranyl ions are bridged through peroxo groups that are bidentate to the uranyl ions, or through pairs of hydroxyl groups. These clusters self-assemble in alkaline aqueous solution only, at a pH of 9 or above. Providing ligands that can bridge uranyl ions in place of the

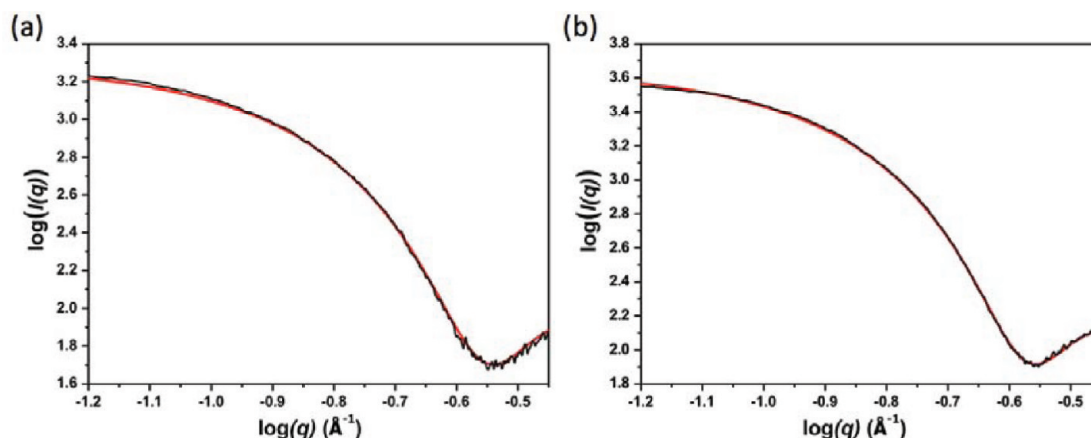


**Figure 4.** Small-angle X-ray scattering data for solutions of (a)  $\text{U}_{50}\text{Ox}_{20}$  and (b)  $\text{U}_{120}\text{Ox}_{90}$  created by dissolving single crystals of the clusters in ultrapure water. The black line shows the data, and the model fit is given in red.

pairs of hydroxyl groups of such clusters permits self-assembly at a lower pH. For example, formation of the oxalate-incorporated  $\text{U}_{50}\text{Ox}_{20}$  occurs at a pH of 5.2–5.6. The  $\text{U}_{50}\text{Ox}_{20}$  still retains four bridges through pairs of hydroxyl groups and is the only cluster we have studied to date containing hydroxyl–hydroxyl bridges that formed below a pH of  $\sim 9$ .

We previously isolated crystals containing the  $\text{U}_{60}\text{Ox}_{30}$  cluster,<sup>20</sup> which corresponds chemically and topologically to the core of the  $\text{U}_{120}\text{Ox}_{90}$  cluster. The smaller cluster was synthesized from an aqueous solution containing uranyl nitrate, peroxide, tetramethylammonium hydroxide,  $\text{K}_2\text{S}_2\text{O}_7$ , and oxalic acid, with a starting pH of 5.8. In the case of  $\text{U}_{120}\text{Ox}_{90}$ , LiOH was used as a base, rather than tetramethylammonium hydroxide, the proportion of oxalic acid relative to uranium was higher, and the starting pH was 6.7. Chemical analysis revealed significant Li in crystals of  $\text{U}_{120}\text{Ox}_{90}$ , and the higher proportion of oxalate relative to uranium is consistent with the dual role of oxalate groups in  $\text{U}_{120}\text{Ox}_{90}$ , where they bridge between uranyl ions in the core and are terminal ligands of uranyl polyhedra in the shell.

Although further studies will be required to determine the details of the assembly mechanism of the  $\text{U}_{120}\text{Ox}_{90}$  cluster, it is apparent that five-membered rings of uranyl pentagonal bipyramids first must assemble in solution. Other types of rings of polyhedra presumably also form, but the presence of abundant K cations in our reactions favors the persistence of topological pentagonals over squares or hexagons.<sup>24</sup> The core structure,  $\text{U}_{60}\text{Ox}_{30}$ , self-assembles as it did in our earlier synthesis, followed by the condensation of the shell, which is directed through bonds to K cations that link to the outer sides of rings of pentagons in the core. As such, the topology of the shell is templated by the core, and the K counterions assume a structure-directing role.

A potential application for nanoscale clusters of uranyl (or other actinide) polyhedra is in separations of uranium from complex solutions, such as in reprocessing of various types of nuclear materials. Currently, actinides are generally separated from other cations in solution through solvent extraction or ion-exchange processes.<sup>31</sup> As the mass and size of cage clusters of uranyl polyhedra are generally much higher than other species in solution, it may be possible to extract such clusters from solution using filtration on the basis of size or mass. The  $\text{U}_{120}\text{Ox}_{90}$  cluster could be particularly suited to such a

hypothetical process because it is both the largest and heaviest cluster containing uranyl that has been reported.

With possible applications of cage clusters of uranyl polyhedra in an advanced nuclear energy system in mind, we have synthesized and characterized dozens of novel clusters.<sup>30</sup> Almost all of these self-assemble in aqueous solution at room temperature. Counter ions and pH are the most important variables for deriving different topologies. Ongoing studies are focusing on the assembly mechanisms, properties, and energetics of such materials using a combination of computational and experimental approaches. This study supports our overall goals by expanding the cluster mass and size range, as well as the pH conditions for self-assembly. Cluster  $\text{U}_{120}\text{Ox}_{90}$  is also a rare example of a core–shell cluster in which the core topology has templated the topology of the shell. Indeed, core–shell topologies are rare in polyoxometalates generally.<sup>32</sup>

## ■ ASSOCIATED CONTENT

### ● Supporting Information

Crystallographic details are provided in a separate file containing tables for each compound. CIF files are available online. This material is available free of charge via the Internet at <http://pubs.acs.org>.

## ■ AUTHOR INFORMATION

### Corresponding Author

\*E-mail: [pburns@nd.edu](mailto:pburns@nd.edu).

### Notes

The authors declare no competing financial interest.

## ■ ACKNOWLEDGMENTS

This material is based upon work supported as part of the *Materials Science of Actinides* Center, an Energy Frontier Research Center funded by the U.S. Department of Energy, Office of Science, Office of Basic Energy Sciences under Award Number DE-SC0001089.

## ■ REFERENCES

- (1) Muller, A.; Serain, C. *Acc. Chem. Res.* **2000**, *33*, 2.
- (2) Long, D. L.; Burkholder, E.; Cronin, L. *Chem. Soc. Rev.* **2007**, *36*, 105.
- (3) Long, D. L.; Tsunashima, R.; Cronin, L. *Angew. Chem., Int. Ed.* **2010**, *49*, 1736.



- (4) Mizuno, N.; Yamaguchi, K.; Kamata, K. *Coord. Chem. Rev.* **2005**, *249*, 1944.
- (5) Gaunt, A. J.; May, I.; Copping, R.; Bhatt, A. I.; Collison, D.; Fox, O. D.; Holman, K. T.; Pope, M. T. *Dalton Trans.* **2003**, 3009.
- (6) Hill, C. L. *J. Mol. Catal. A: Chem.* **2007**, *262*, 2.
- (7) Mal, S. S.; Dickman, M. H.; Kortz, U. *Chem.—Eur. J.* **2008**, *14*, 9851.
- (8) Mitchell, S. G.; Streb, C.; Miras, H. N.; Boyd, T.; Long, D. L.; Cronin, L. *Nature Chem.* **2010**, *2*, 308.
- (9) Muller, A.; Peters, F.; Pope, M. T.; Gatteschi, D. *Chem. Rev.* **1998**, *98*, 239.
- (10) Pradeep, C. P.; Long, D. L.; Cronin, L. *Dalton Trans.* **2010**, *39*, 9443.
- (11) Yan, J.; Gao, J.; Long, D. L.; Miras, H. N.; Cronin, L. *J. Am. Chem. Soc.* **2010**, *132*, 11410.
- (12) Duval, P. B.; Burns, C. J.; Clark, D. L.; Morris, D. E.; Scott, B. L.; Thompson, J. D.; Werkema, E. L.; Jia, L.; Andersen, R. A. *Angew. Chem., Int. Ed.* **2001**, *40*, 3357.
- (13) Soderholm, L.; Almond, P. M.; Skanthakumar, S.; Wilson, R. E.; Burns, P. C. *Angew. Chem., Int. Ed.* **2008**, *47*, 298.
- (14) Burns, P. C.; Kubatko, K. A.; Sigmon, G.; Fryer, B. J.; Gagnon, J. E.; Antonio, M. R.; Soderholm, L. *Angew. Chem., Int. Ed.* **2005**, *44*, 2135.
- (15) Forbes, T. Z.; McAlpin, J. G.; Murphy, R.; Burns, P. C. *Angew. Chem., Int. Ed.* **2008**, *47*, 2824.
- (16) Ling, J.; Qiu, J.; Szymanowski, J. E. S.; Burns, P. C. *Chem.—Eur. J.* **2011**, *17*, 2571.
- (17) Ling, J.; Wallace, C. M.; Szymanowski, J. E. S.; Burns, P. C. *Angew. Chem., Int. Ed.* **2010**, *49*, 7271.
- (18) Sigmon, G.; Ling, J.; Unruh, D. K.; Moore-Shay, L.; Ward, M.; Weaver, B.; Burns, P. C. *J. Am. Chem. Soc.* **2009**, *131*, 16648.
- (19) Sigmon, G. E.; Burns, P. C. *J. Am. Chem. Soc.* **2011**, *133*, 9137.
- (20) Sigmon, G. E.; Unruh, D. K.; Ling, J.; Weaver, B.; Ward, M.; Pressprich, L.; Simonetti, A.; Burns, P. C. *Angew. Chem., Int. Ed.* **2009**, *48*, 2737.
- (21) Sigmon, G. E.; Weaver, B.; Kubatko, K. A.; Burns, P. C. *Inorg. Chem.* **2009**, *48*, 10907.
- (22) Unruh, D. K.; Burtner, A.; Pressprich, L.; Sigmon, G.; Burns, P. C. *Dalton Trans.* **2010**, *39*, 5807.
- (23) Unruh, D. K.; Ling, J.; Qiu, J.; Pressprich, L.; Baranay, M.; Ward, M.; Burns, P. C. *Inorg. Chem.* **2011**, *50*, 5509.
- (24) Miro, P.; Pierrefixe, S.; Gicquel, M.; Gil, A.; Bo, C. *J. Am. Chem. Soc.* **2010**, *132*, 17787.
- (25) Vlaisavljevich, B.; Gagliardi, L.; Burns, P. C. *J. Am. Chem. Soc.* **2010**, *132*, 14503.
- (26) Sheldrick, G. M. *SHELXTL*; Bruker AXS, Inc.: Madison, WI, 1996.
- (27) Cejka, J. *Rev. Mineral.* **1999**, *38*, 521.
- (28) Petrov, I.; Soptrajanov, B. *Spectrochim. Acta, Part A* **1975**, *A 31*, 309.
- (29) Burns, P. C.; Ewing, R. C.; Hawthorne, F. C. *Can. Mineral.* **1997**, *35*, 1551.
- (30) Burns, P. C. *Mineral. Mag.* **2011**, *75*, 1.
- (31) Nash, K. L.; Madic, C.; Mathur, J. N.; Lacquement, J. In *The Chemistry of the Actinide and Transactinide Elements*; Morss, L. R., Edelstein, N. M., Fuger, J., Katz, J. J., Eds.; Springer: Dordrecht, the Netherlands, 2006; p 2622.
- (32) Fang, X. K.; Kogerler, P.; Furukawa, Y.; Speldrich, M.; Luban, M. *Angew. Chem., Int. Ed.* **2011**, *50*, 5212.